

Strong focusing properties and far-field focus in the two-dimensional photonic-crystal-based concave lens

Renlong Zhou, Xiaoshuang Chen,^{*} and Wei Lu[†]*National Laboratory for Infrared Physics, Shanghai Institute of Technical Physics, Chinese Academy of Sciences, 200083 Shanghai, People's Republic of China*

(Received 30 October 2005; revised manuscript received 26 April 2006; published 27 July 2006)

We have demonstrated that the strong and far-field focusing of a point source and a plane wave in a two-dimensional photonic-crystal-based concave lens by the use of the standard finite-difference time-domain simulations. The effect of the distance between the point source and the lens on the focusing is discussed. The far-field focus of a plane wave is shown. In addition, a plane wave is formed with placing the source at the focus point. According to the calculation, the strong and good quality far-field focusing of the transmitted wave, explicitly following the well-known wave beam negative refraction law, can be realized. Moreover, the spatial frequencies information of the Bloch mode in multiple Brillouin zones is investigated in order to indicate the wave propagation in two different regions.

DOI: [10.1103/PhysRevE.74.016610](https://doi.org/10.1103/PhysRevE.74.016610)

PACS number(s): 42.79.-e, 42.25.-p, 41.20.Jb, 78.20.Ci

I. INTRODUCTION

The existence and impact of left-handed materials (LHM) was pointed out by Veselago [1]. Years later, some theoretical and experimental groups investigated the LHM for investigating a number of unusual electromagnetic effects [2–17]. The phase velocity of the light wave propagating inside this medium is pointed in the opposite direction of the energy flow. Thus, the Poynting vector and wave vector are antiparallel. Consequently, the light is refracted negatively. Parimi *et al.* have demonstrated the imaging by a planar photonic crystal (PC) flat lens by using negative refraction [7]. The results have shown that such a lens can focus a point source on one side of the lens into a real point image on the other side. The focusing effect is observed for frequency ranges at which the wave vector of the incident waves and the group velocity of the transmitted waves fall into the opposite sides of the interface normal by analyzing the equifrequency-surface contours (EFCs) of the band structures [11,12]. As a result, for such frequency ranges the PC behaves as if the index of refraction is negative. In particular, Luo *et al.* have demonstrated a frequency range in which one can obtain a single negative-refractive beam for all incident angles in the lowest photonic band close to the band edge [8]. The negative refraction in the lowest band close to the band edge may be more desirable in obtaining high-resolution transmission and single-mode behavior. However, such a so-called focusing effect has only been found in the near-field region. The near-field focusing operates only when the source is close to the lens [7–10,20]. For a majority of applications of lenses far-field focusing is required.

In recent work, research shows [17] that good-quality non-near-field images and focusing have been observed in the two-dimensional coated PC with triangular lattice for the electromagnetic waves or by adding an additional component to the existing photonic crystal. In addition, the far-field focusing of acoustic waves has also been shown in two-

dimensional sonic crystals consisting of hexagonal arrays of steel cylinders in air [18]. In further research, negative refraction allows the focusing of a far-field radiation by concave rather than convex surfaces [19,22] with the advantage of reduced aberration for the same radius of curvature and changes many commonly accepted aspects of conventional optical systems. One prominent example towards far-field focusing has been experimentally realized in a planoconcave lens by Vodo and Parimi *et al.* [22]. In addition, the focusing using a planoconcave lens made of a left-handed metamaterial with interleaving arrays of wire strips and split ring resonators has also been demonstrated experimentally by Parazzoli *et al.* [21]. The possible applications of such a phenomenon to photonic devices are anticipated.

In this paper, we propose a two-dimensional (2D) photonic-crystal-based concave lens to realize the strong and far-field focusing effect. The waves emerge from the background material, propagating through a section of a PC designed for negative refraction at the considered frequency range, and exiting to the background material. The effect of the distance between the point source and the lens on the focusing is discussed. The focusing of a plane wave is successfully observed. According to the calculation, the far-field focusing of a plane wave is obtained. In addition, a plane wave is formed for the source placed at the focus point. Moreover, the spatial frequencies information of the Bloch mode is investigated, describing the wave propagation in the 2D PC concave lens system.

II. FOCUSING PROPERTIES IN THE 2D PHOTONIC-CRYSTAL-BASED CONCAVE LENS

The system we examine is the 2D photonic-crystal-based concave lens consisting of a square lattice of circular air holes (with lattice constant a and hole radius $r=0.35a$) in dielectric background with $\epsilon=12.0$ as shown in Fig. 1(a). The optical principal axis of the lens is normal along the ΓM direction with the length $AB=16.9a$, and the curvature of the lens is 0.7092. Here the point A (B) is located at the left (right) surface along the optical principal axis. Only TE

^{*}Corresponding author. Email address: xschen@mail.sitp.ac.cn

[†]Corresponding author. Email address: luwei@mail.sitp.ac.cn

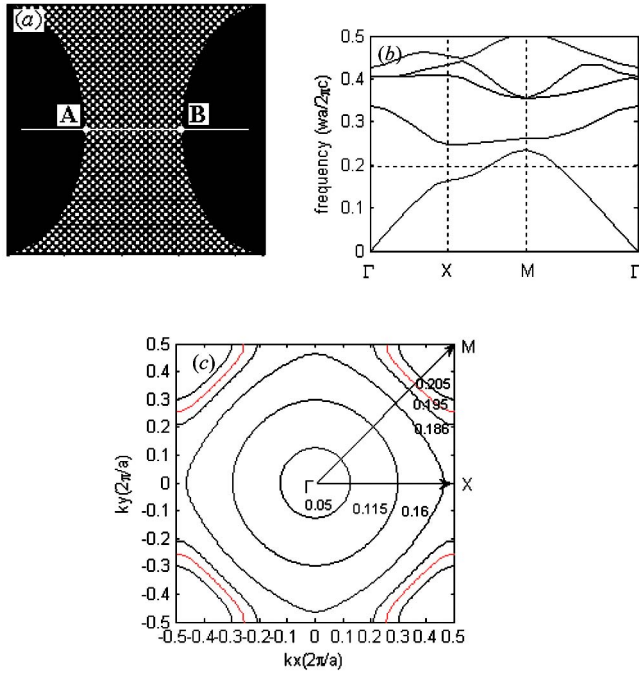


FIG. 1. (Color online) (a) The photonic-crystal-based concave lens; (b) band structure of the PC calculated with the plane wave expansion method; (c) the EFCs of the first band for the TE polarization mode. Frequency values are in units of $2\pi c/a$.

modes (magnetic field parallel to the axis of the holes) are considered.

To visualize and analyze the negative refractive effect and the far-field focusing, by using a plane-wave expansion method [8,23], we have calculated the photonic band structure in Fig. 1(b) and the EFCs in Fig. 1(c) for the TE mode in \vec{k} space whose gradient vectors give the group velocities of the photonic modes. In Fig. 1(c), the EFCs for five relevant frequencies are demonstrated, respectively. Note that throughout this paper the frequency is always in a units of $2\pi c/a$. The 0.05 and 0.115 contours are very close to a perfect circle, and therefore the group velocity at any point of the contour is collimated with the \vec{k} vector and $\vec{k} \cdot \partial\omega / \partial\vec{k} \geq 0$, indicating that the crystal behaves like an effective homogeneous medium with a positive effective index for two long wavelengths. The contour with frequency 0.16 is a bit distortion from a circle, with the distance $|\vec{k}|$ along the ΓM direction slightly shorter than along the ΓX direction, indicating

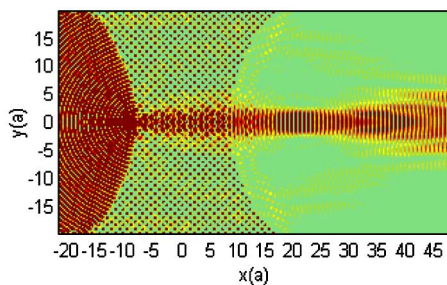


FIG. 2. (Color online) A point source placed at $x = -8.84a$ is incident to the photonic-crystal-based concave lens, and a snapshot of the wave propagation is at the frequency 0.195.

that the crystal behaves like a positive effective index medium. In most parts of the 0.195 contour, the curve is quite flat in the middle of this contour and has the surface normal pointing to the ΓM direction. In small parts of the 0.195 contour near the Brillouin Zone (BZ) edges, the surface is convex with respect to the M point. For the 0.195 contour, the group velocity of the excited Bloch wave mode near the BZ edges is pointed towards the M point, corresponding to an apparent negative refraction direction. And the group velocity centered around the ΓM direction in most parts of the 0.195 contour would point dominantly along the ΓM direction.

III. FOCUSING PROPERTIES OF A POINT SOURCE

The finite difference time domain (FDTD) approach has been used to calculate the propagation of an electromagnetic (EM) wave emitted from a monochromatic TE-polarized point source with the frequency 0.195. The geometry of the photonic-crystal-based concave lens is displayed in Fig. 2. The center of the concave lens along the optical principal axis is always set to $x=0$, and the concave lens is symmetric with respect to $y=0$. A typical intensity distribution ($|H_z|^2$) is also shown in Fig. 2. The point source is placed at $x = -8.84a$ and $y=0$, very close to the surface of the concave lens. First, the beam rapidly focuses at its entry region inside the PC. Then, the beam spreads inside the PC, and focuses again after it exits to the background material region. A clear signature of the negative refraction effect for those large angle wave components near the right region is shown in Fig. 2 [9]. One can also find that the focused beam is distorted due to the nonideal circular shape of EFS in the photonic crystal structure. So an incoming wave with the frequency 0.195 can propagate into this crystal along or close to the ΓM direction [24].

Assuming that the propagating power is mainly coupled to the zero-order diffracted wave, we can apply Snell's law [$n(\omega, k_i) \sin \theta_r = n_{e_a} \sin \theta_i$], where θ_i is the angle of incidence in the background material, and θ_r is the angle of refraction inside the PC. The $n(\omega, k_i)$ is the refractive index along the propagation direction k_i and n_{e_a} is the refractive index of the background material. The advantage of refraction of the first band close to the band edge is the single-beam propagation and high transmission efficiency because the curve is quite flat in most parts of the 0.195 contour with the surface normal pointing to the ΓM direction. So we avoid suffering from Bragg reflections that take place inside the photonic crystal. The result has indicated that a well-defined single-beam propagation is negatively refracted rather than multiple Bragg waves propagating in different directions of the PC. These can help us to design lenses and realize the focusing of the wave.

By changing the distance between the source and the concave lens, we intend to know what happens to the focusing effect. A schematic picture of the structure is shown in Fig. 3(a). The intensity distributions for a point source with three different positions $x = -75a$, $x = -65a$, and $x = -22a$ are displayed in Figs. 3(b)–3(d), respectively. For the sources in the far-field domain of Figs. 3(b) and 3(c), the beam transmits

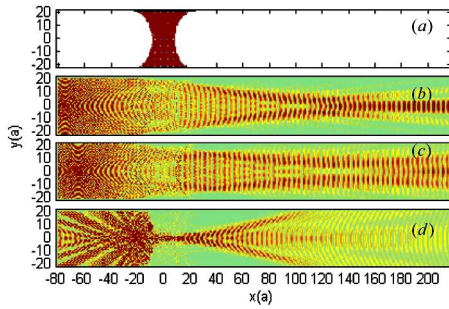


FIG. 3. (Color online) (a) The schematic picture of the structure. A snapshot of the wave propagation is at the frequency 0.195 with a point source at different positions: (b) $x=-75a$, (c) $x=-65a$, and (d) $x=-22a$, respectively.

into the left surface in accordance with Snell's law and the wave transmitting inside the concave lens is propagating along or close to the ΓM direction. In the right surface region, we can clearly see that light intensity is in good agreement with the wave beam negative refraction law. As shown in Fig. 3(c), a plane wave is formed near the right surface. For the source near the left surface of PC in Fig. 3(d), the beam rapidly focuses at its entry region inside the PC, and then spreads after it exits to the background material section. The shape of the above three intensity distributions, showing how the EM wave transmits through the PC, is different from each other due to the different positions of the sources. An incoming wave can propagate into this crystal along or close to the ΓM [(11)] direction. This result is also consistent with the EFCs analysis in Fig. 1(c).

To analyze in more detail the focusing behavior for the point source, the transversal (y direction) light intensity is shown in Fig. 4 for seven positions $x/a=-8.45, -4.23, 0, 4.23, 8.45, 16,$ and 213 corresponding to the point source placed at three different positions (a) $x=-75a$, (b) $x=-65a$, and (c) $x=-22a$, respectively. For the source placed in the far-field domain in Figs. 4(a) and 4(b), one can see that the light intensity shows the focusing behaviors clearly. In the

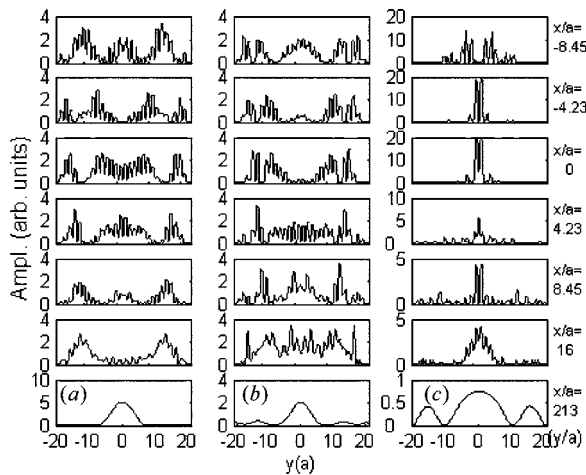


FIG. 4. Intensity distributions along the transverse (y) direction at seven positions correspond to the point source placed at three different positions: (a) $x=-75a$, (b) $x=-65a$, and (c) $x=-22a$, respectively.

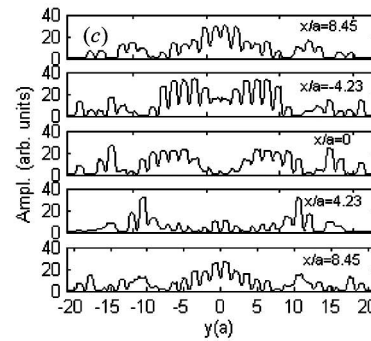
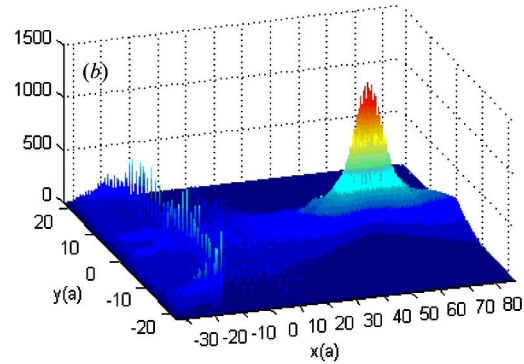
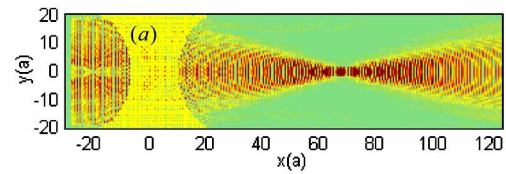


FIG. 5. (Color online) (a) The intensity distribution and (b) the surface of the field distribution for a plane wave incident to the PC interface. A high quality far-field focus is formed out of the concave lens. (c) Intensity distributions along the transverse direction at five positions.

region near the surface, the focusing behaviors occur mainly due to the negative refractive effect. The transmission of the waves inside the concave lens is along or close to the ΓM [(11)] direction. For the source placed very close to the interface of PC, as shown in Fig. 4(c), the light intensity is mainly focused along the ΓM direction inside the PC, and then spreads after the beam exits to the background material section.

IV. FOCUSING PROPERTIES OF A PLANE WAVE

For the photonic-crystal-based thin lab lens, only the near-field focusing is easily observed. In the photonic-crystal-based concave lens, we can find that the far-field focusing is formed. We perform a simulation for the incident plane wave at frequency $\omega=0.195(2\pi c/a)$. A typical result of the intensity distribution is shown in Fig. 5(a) and the strong focusing of the waves is successfully observed. The surface of the field distribution for a plane wave incident to the PC surface is also shown in Fig. 5(b). One can find easily that a far-field focusing of the plane wave is formed out of the PC concave

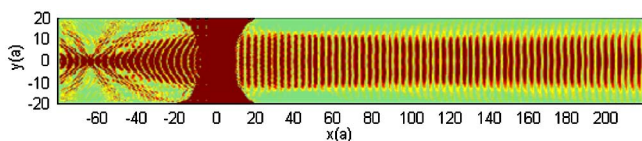


FIG. 6. (Color online) A line source at the focal point incident to the PC interface with frequency 0.195 and a width $4.5a$. A well-shaped plane wave is obtained.

lens, and the focusing keeps on in a steady state. The focal point is centered at $x=65a$ and $y=0$, that is, the focal length is $65a$ and it is very far from the right interface of the concave lens. The strong focal point has a width maximum of $4.5a$. The intensity of the focusing is three times stronger than that of the incident plane wave. The results confirm that far-field focusing is realizable and opens the door for the applications of the LHM in the far-field region.

Next, in order to discuss in more detail the focusing effect of the plane wave source, the transversal (y direction) light intensities at five positions $x/a=-8.45, -4.23, 0, 4.23, 8.45$ are shown in the Fig. 5(c), respectively. It is found that the intensity distribution in the $x/a=-8.45$ and $x/a=8.45$ is symmetric with respect to $x=0$. The intensity distribution along y shows how the EM wave transmits through the PC concave lens. In the left and right surface regions, we can clearly see that light intensity is in good agreement with the wave beam negative refraction law. The wave with the frequency 0.195 propagating inside the PC concave lens is along the ΓM direction. The focusing behavior is in complete agreement with the analysis on the EFCs analysis.

When a point source is placed at the focal point and incident to the PC interface with frequency 0.195, a well-shaped plane wave is obtained, as shown in Fig. 3(c). Furthermore, as shown in Fig. 6, we have placed a line source instead of a point source with the full width $4.5a$ at the focus point $x=-65a$ and $y=0$. Then, a plane wave is well formed out of the PC concave lens. In a recent paper [22], Vodo and Parimi *et al.* have studied the focusing behavior by a planoconcave lens. In comparison with their results, some similar focusing effects are shown, such as the far-field focusing of a plane wave and a plane wave being produced from a source [22].

Furthermore, at a given frequency 0.195 inside the PC concave lens, the propagation behaviors can be explained by means of the spatial Fourier spectrum. As shown in Fig. 7, for one particular y , a spatial Fourier transform of the field data presented in Fig. 5(a) along the x direction, around the focus region, and inside the PC concave lens region, yields the spectrum $F(k_x)$ of the spatial frequency k_x [9,25]. Spatial frequency kx are in units of $2\pi/(\sqrt{2}a)$. To improve signal-to-noise ratio, the spectra $F(k_x)$ are summed for all y . We can find that the Bloch mode, which consists of more than one spatial frequency, is visualized in the Fig. 7. These spatial frequencies are separated by an integral number of $\pi/(\sqrt{2}a)$ along the ΓM direction for the square lattice, as seen in Fig. 7 for the first five zones. At frequency 0.195, the intensity of the Bloch harmonics for the same Bloch mode inside the PC region with $k_x=0.705$ and 1.295 can be given as peaks (dotted line) in Fig. 7. One can find that the amplitudes of Bloch harmonics separated by $\pi/(\sqrt{2}a)$ are different. The exact physical interpretation behind this observation has been

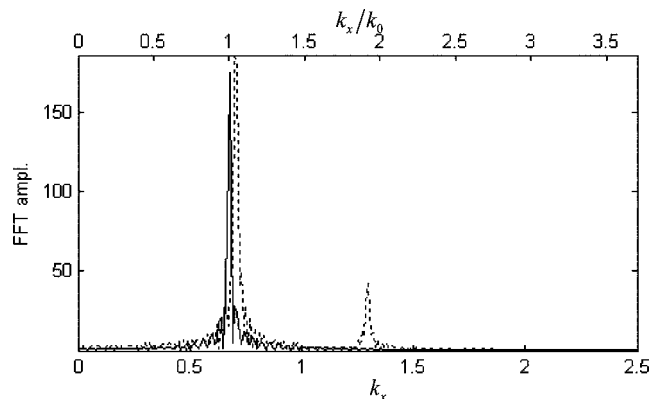


FIG. 7. Spatial Fourier spectrum $F(kx)$ versus spatial frequency kx for frequency 0.195 is summed around the focus region (solid line) and inside the PC concave lens region (dotted line) corresponding to the field data presented in Fig. 5(a).

shown in Ref. [25]. As shown in Fig. 7, near the focus region, only the Bloch mode $k_x=k_0=0.195\sqrt{12}$ (k_0 is the wave number at the frequency 0.195 in the dielectric background) with frequency 0.195 contributes to the propagation of the EM wave. Therefore, when the waves leave the PC concave lens, the focusing of the waves is formed [24].

V. CONCLUSION

We have realized the strong and far-field focusing of a point source and a plane wave by a 2D photonic-crystal-based concave lens with the standard finite-difference time-domain technique. The far-field focus of a plane wave is obtained out of the concave lens, while a plane wave is also formed for the source placed at the focus point. In comparison with the results of Vodo and Parimi, some similar focusing effects are shown, such as the far-field focusing of a plane wave and a plane wave being produced from a source [22]. In addition, in our 2D photonic-crystal-based concave lens, the strong and far-field focusing of a point source has also been found. The effect of the distance between the point source and the lens on the focusing is shown. Moreover, the spatial frequencies information of the Bloch mode in multiple Brillouin zones is investigated, demonstrating the wave propagation in the 2D PC concave lens system. Focusing is expected to be a significant step towards novel imaging optics and can lead to considerable changes in optical system design [26]. It could also make possible three-dimensional photography and novel coupling functionality in integrated optics components.

ACKNOWLEDGMENTS

This work was supported in part by the Chinese National Key Basic Research Special Fund, the Key Fund of Chinese National Science Foundation (Grant No. 10234040), Chinese National Science Foundation (Grants No. 60476040 and No. 60576068), Grand Foundation of Shanghai Science and Technology (Grant No. 05DJ14003), and the computational support from Shanghai Supercomputer Center.

- [1] V. G. Veselago, *Sov. Phys. Usp.* **10**, 509 (1968).
- [2] R. A. Shelby, D. R. Smith, and S. Schultz, *Science* **292**, 77 (2001); D. R. Smith, D. Schurig, J. J. Mock, P. Kolinko, and P. Rye, *Appl. Phys. Lett.* **84**, 2244 (2004).
- [3] C. G. Parazzoli, R. B. Greigor, K. Li, B. E. C. Koltenbah, and M. Tanielian, *Phys. Rev. Lett.* **90**, 107401 (2003).
- [4] J. B. Pendry, *Phys. Rev. Lett.* **85**, 3966 (2000); A. A. Houck, J. B. Brock, and I. L. Chuang, *ibid.* **90**, 137401 (2003); S. A. Ramakrishna and J. B. Pendry, *Phys. Rev. B* **67**, 201101(R) (2003).
- [5] P. V. Parimi, W. T. Lu, P. Vodo, J. Sokoloff, J. S. Derov, and S. Sridhar, *Phys. Rev. Lett.* **92**, 127401 (2004).
- [6] E. Cubukcu, K. Aydin, E. Ozbay, S. Foteinopoulou, and C. M. Soukoulis, *Nature (London)* **423**, 604 (2003); A. Grbic and G. V. Eleftheriades, *Phys. Rev. Lett.* **92**, 117403 (2004).
- [7] P. V. Parimi, W. T. Lu, P. Vodo, and S. Sridhar, *Nature (London)* **426**, 404 (2003).
- [8] C. Luo, S. G. Johnson, J. Joannopoulos, and J. Pendry, *Phys. Rev. B* **65**, 201104(R) (2002); Z. Ruan, M. Qiu, S. Xiao, S. He, and L. Thylen, *ibid.* **71**, 045111 (2005); S. Feng *et al.*, *ibid.* **72**, 075101 (2005).
- [9] S. He *et al.*, *Phys. Rev. B* **70**, 115113 (2004); C. Luo, S. G. Johnson, J. D. Joannopoulos, and J. B. Pendry, *ibid.* **68**, 045115 (2003); S. Xiao, Z. Ruan, M. Qiu, and S. He, *ibid.* **85**, 4269 (2004).
- [10] E. Cubukcu, K. Aydin, E. Ozbay, S. Foteinopoulou, and C. M. Soukoulis, *Phys. Rev. Lett.* **91**, 207401 (2003).
- [11] Alejandro Martínez and Javier Martí, *Opt. Express* **13**, 2858 (2005).
- [12] A. A. Houck, J. B. Brock, and I. L. Chuang, *Phys. Rev. Lett.* **90**, 137401 (2003); E. J. Reed, M. Soljacic, and J. D. Joannopoulos, *Phys. Rev. Lett.* **91**, 133901 (2003).
- [13] S. Enoch, G. Tayeb, and B. Gralak, *IEEE Trans. Antennas Propag.* **51**, 2659 (2003).
- [14] S. Foteinopoulou, E. N. Economou, and C. M. Soukoulis, *Phys. Rev. Lett.* **90**, 107402 (2003).
- [15] C.-H. Kuo and Z. Ye, *Phys. Rev. E* **70**, 056608 (2004).
- [16] Z. Y. Li and L. L. Lin, *Phys. Rev. B* **68**, 245110 (2003).
- [17] X. Zhang, *Phys. Rev. E* **71**, 037601 (2005); X. Zhang, *Phys. Rev. B* **71**, 165116 (2005).
- [18] L. Feng, X. P. Liu *et al.*, *Phys. Rev. B* **72**, 033108 (2005).
- [19] J. B. Pendry and D. R. Smith, *Phys. Today* **57**, 37 (2004); Alejandro Martínez and Javier Martí, *Opt. Express* **13**, 2858 (2005).
- [20] C. Luo, M. Ibanescu, S. G. Johnson, and J. D. Joannopoulos, *Science* **299**, 368 (2003); X. Hu and C. T. Chan, *Appl. Phys. Lett.* **85**, 1520 (2004).
- [21] C. G. Parazzoli, R. B. Greigor, J. A. Nielsen, M. A. Thompson, K. Li, A. M. Vetter, M. H. Tanielian, and D. C. Vier, *Appl. Phys. Lett.* **84**, 3232 (2004).
- [22] P. Vodo, P. V. Parimi, W. T. Lu, and S. Sridhar, *Appl. Phys. Lett.* **86**, 201108 (2005).
- [23] K. M. Ho, C. T. Chan, and C. M. Soukoulis, *Phys. Rev. Lett.* **65**, 3152 (1990).
- [24] M. Qiu, Lars Thylen, Marcin Swillo, and Bozena Jaskorzynska, *IEEE J. Quantum Electron.* **9**, 106 (2003); A. Berrier, M. Mulot, M. Swillo, M. Qiu, L. Thylen, A. Talneau, and S. Anand, *Phys. Rev. Lett.* **93**, 073902 (2004).
- [25] H. Gersen *et al.*, *Phys. Rev. Lett.* **94**, 123901 (2005); **94**, 073903 (2005).
- [26] P. Vodo, P. Parimi, W. T. Lu, S. Sridhar, and R. Wing, *Appl. Phys. Lett.* **85**, 1858 (2004).